

How to reliably estimate collapsing-threshold diffusion model parameters? A simulation study

Amir Hosein Hadian Rasanan¹, Lukas Schumacher¹, Michael D. Nunez², Gabriel Weindel³, Jörg Rieskamp¹

¹ Department of Psychology, University of Basel, Basel, Switzerland

² Psychological Methods, University of Amsterdam, Amsterdam, The Netherlands

³ Department of Experimental Psychology, Utrecht University, Utrecht, The Netherlands

Abstract

Evidence accumulation models have become the dominant theory in explaining neural and behavioral constructs of decision-making. The main principle of these models is that a decision-maker accumulates noisy evidence until a constant threshold is reached. However, several behavioral and neuroscientific findings, besides some theoretical motivations like optimality, have led to alternative proposals, such as “collapsing threshold” models. Usually, these models offer a more accurate fit to empirical data. However, a major issue with these models is the unreliability of parameter estimation. Due to this, researchers have relied solely on model fit comparisons, avoiding interpretation of the parameter values – leading to controversial findings in the literature that support these models. This work introduces a reliable model estimation framework by linking the non-decision time to external measurements. In this modeling framework, we consider a joint likelihood function for behavioral measurements and the non-decision time measurement, constraining the non-decision time estimation. The results of a parameter recovery study showed that the proposed joint model makes the collapsing threshold parameters identifiable.

Keywords: Collapsing threshold; Decision making; Evidence accumulation models; Joint modeling; Parameter estimation

Introduction

Collapsing threshold diffusion models (CT-DDM) are a class of diffusion decision models (DDM; Ratcliff, 1978) in which the decision threshold can vary as time passes. These models have several key advantages over fixed threshold diffusion models, such as predicting Gaussian-like response time (RT) distributions (Evans & Hawkins, 2019; Hawkins et al., 2015), providing a normative optimal decision policy (Fudenberg et al., 2018; Frazier & Yu, 2007; Drugowitsch et al., 2012; Tajima et al., 2016), and consistency with neuroscience findings on urgency (Thura et al., 2012; Cisek et al., 2009; Murphy et al., 2016). The evidence accumulation process in this model can be represented by a Wiener process as follows:

$$dX(t) = \delta dt + s dW(t), \quad b_l(0) < X(0) = x_0 < b_u(0), \quad (1)$$

where $X(t)$ represents the accumulated evidence until time t , δ is the mean evidence accumulation rate (drift rate), s is the diffusion coefficient, x_0 is the starting point bias (also known

as a priori bias), and $dW(t)$ is the Wiener process. The process starts the accumulation from x_0 and continues until the accumulator crosses either the upper ($b_u(t)$) or lower ($b_l(t)$) threshold (i.e., $X(t) \geq b_u(t)$ or $X(t) \leq b_l(t)$). These mechanisms are a part of the decision process and predict decision time. However, RT also contains some components unrelated to the decision process, such as perceptual encoding and motor execution. To exclude the effect of these components from RT, DDM also contains a non-decision time parameter (τ), which is assumed to correspond to the duration of all decision-unrelated processes.

Despite all the theoretical benefits of collapsing threshold diffusion models, several systematic assessments employing various parameter estimation methods (see Hadian Rasanan et al., 2023, for a discussion on various estimation methods) reported poor parameter recovery for these models (Evans et al., 2020; Murrow & Holmes, 2024). However, an accurate parameter recovery is essential for interpreting the parameters of a cognitive model. This situation complicates the interpretation of the model's parameters.

A potential approach for improving the parameter recovery is to employ joint modeling. In other words, linking the model's parameters to additional observations adds constraints to the model's parameters and, as a result, makes them identifiable (Nunez et al., 2025; Ghaderi-Kangavari et al., 2023). Traditionally, we only use RT and choice data to fit DDM and estimate the parameters. However, in this model, we constrain the non-decision time parameter using an additional data source related to non-decision time. This additional data is a trial-level noisy estimation of non-decision time, and we assume that the true non-decision (τ) is the mean value of these observations. Therefore, for each trial, we have a measurement of RT_n , $Choice_n$, and non-decision time (Z_n) as follows:

$$RT_n, Choice_n \sim \text{CT-DDM}(\delta, x_0, b_u(t), b_l(t), \tau),$$

$$\log(Z_n) \sim \mathcal{N}(\mu, \sigma^2).$$

We considered a log-normal distribution with parameters μ and σ for non-decision time observation because the non-decision time is a positively valued random variable with a right-skewed distribution, and neuroimaging studies showed that it is approximately distributed log-normally (Weindel et al., 2021). As mentioned before, we assume that the true non-decision time (τ) is the mean value of the distribution, which implies $\tau = \exp(\mu + \sigma^2/2)$ or equivalently $\mu = \log(\tau) - \frac{\sigma^2}{2}$. A potential way of estimating the non-decision time at the trial

level is to extract it from neural signal data (e.g., Weindel et al., 2024; Nunez et al., 2019; Weindel et al., 2021).

Simulation procedure

We conducted a parameter recovery study based on 1000 simulation data sets to test whether we can estimate the parameters of the joint model reliably. We considered two different dynamics for the threshold, the hyperbolic and the exponential functions, as follows:

$$b_u(t) = \theta \times \exp(-\lambda t), \quad \text{or} \quad b_u(t) = \frac{\theta}{1 + \lambda t},$$

where θ is the starting threshold (i.e., $b_u(0) = \theta$) and $\lambda > 0$ is the decay rate. $b_u(t)$ stands for the upper threshold, and the lower threshold is equal to the reflection of the upper threshold (i.e., $b_l(t) = -b_u(t)$). In all simulations, we assumed that the accumulation process starts from zero (i.e., starting point $x_0 = 0$). Also, we set the diffusion coefficient equal to one (i.e., $s = 1$). To simulate RT and choice, we considered the discrete form of the accumulation process (1) with a time step $\Delta t = 0.001$. To cover a wide range of model behavior in the simulations, we considered the following distributions for the model parameters: $\theta \sim \mathcal{U}[1.5, 4]$, $\lambda \sim \mathcal{U}[0.1, 2]$, $\delta \sim \mathcal{U}[0, 3]$, $\tau \sim \mathcal{U}[0.05, 1]$, and $\sigma \sim \mathcal{U}[0.1, 1]$.

After generating 1000 random parameter sets from the above distributions, we generated RT, choice, and noisy non-decision time observation for 500 trials. As mentioned, we assumed that the non-decision time is the mean value of a log-normal distribution. Then, the location parameter of the log-normal distribution is obtained by $\mu = \log(\tau) - \frac{\sigma^2}{2}$. Therefore, in each trial, we sampled a noisy observation of non-decision time using the following log-normal distribution (i.e., $\log(Z_n) \sim \mathcal{N}(\log(\tau) - \frac{\sigma^2}{2}, \sigma^2)$). To compare the quality of parameter recovery with the pure behavioral model (the No-constraint model), we conducted the same simulation study for CT-DDM without informing the model of non-decision time observations.

We used the integral equation method to approximate the likelihood function of the collapsing threshold diffusion model Smith & Ratcliff (2022); Smith (2000). Also, we have employed the differential evolution optimization routine to minimize the joint negative log-likelihood. To evaluate the precision of parameter recovery, we employed the r-squared index $R^2 = 1 - \frac{\sum_{i=1}^N (\vartheta_i - \hat{\vartheta}_i)^2}{\sum_{i=1}^N (\vartheta_i - \bar{\vartheta})^2}$, in which ϑ and $\hat{\vartheta}$ stand for the true generating parameter and estimated parameter, respectively. Also, $\bar{\vartheta}$ shows the mean of the true parameter.

Simulation results

Figure 1 illustrates the r-squared values for the threshold parameters (i.e., θ and λ) for the No-constraint and NDT-constraint (i.e., the joint model) models. This plot shows a considerable improvement in the precision of parameter recovery for the threshold parameters after considering an additional constraint on non-decision time. This improvement

is more considerable for the Hyperbolic collapsing threshold model.

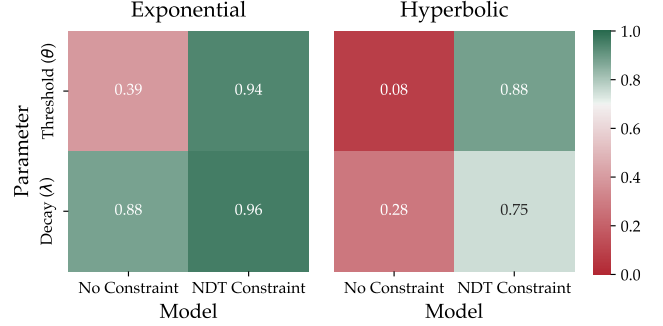


Figure 1: R-squared values for threshold parameters in exponential (left panel) and hyperbolic (right panel) collapsing threshold models.

Figure 2 presents the sensitivity of the parameter recovery to the noise level in non-decision time observation. We simulated data with three standard deviation levels (i.e., $\sigma_z = 0.3, 0.6$, and 0.9) for non-decision time observation. The results show that first, the parameter recovery is still reliable even with a high noise level in non-decision time observation, and second, the parameter recovery of joint models is substantially better than the parameter recovery of the pure behavioral model.

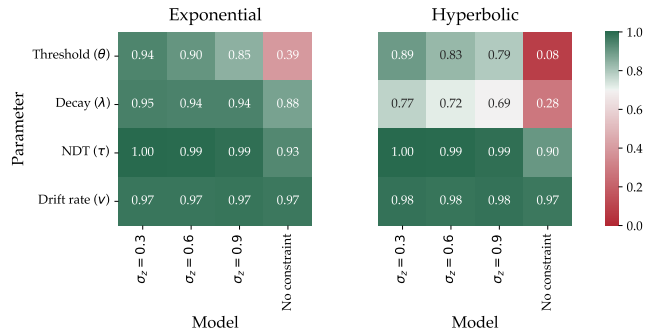


Figure 2: Illustration of sensitivity of parameter estimation to the noise level in the non-decision time observations.

Conclusion

The proposed non-decision time constraint CT-DDM provides a cognitive modeling framework in which all the collapsing threshold parameters are reliably identifiable. Therefore, such joint models allow researchers to interpret parameter values directly, potentially helping to resolve controversial findings in the urgent literature. Moreover, prior research has demonstrated that urgency signal models can be reformulated as collapsing threshold models (Smith & Ratcliff, 2022), indicating that the proposed model is also applicable to urgency-based accounts.

References

- Cisek, P., Puskas, G. A., & El-Murr, S. (2009). Decisions in changing conditions: the urgency-gating model. *Journal of Neuroscience*, 29(37), 11560–11571. doi: 10.1523/JNEUROSCI.1844-09.2009
- Drugowitsch, J., Moreno-Bote, R., Churchland, A. K., Shadlen, M. N., & Pouget, A. (2012). The cost of accumulating evidence in perceptual decision making. *Journal of Neuroscience*, 32(11), 3612–3628. doi: 10.1523/JNEUROSCI.4010-11.2012
- Evans, N. J., & Hawkins, G. E. (2019). When humans behave like monkeys: Feedback delays and extensive practice increase the efficiency of speeded decisions. *Cognition*, 184, 11–18. doi: 10.1016/j.cognition.2018.11.014
- Evans, N. J., Trueblood, J. S., & Holmes, W. R. (2020). A parameter recovery assessment of time-variant models of decision-making. *Behavior Research Methods*, 52, 193–206. doi: 10.3758/s13428-019-01218-0
- Frazier, P., & Yu, A. J. (2007). Sequential hypothesis testing under stochastic deadlines. *Advances in Neural Information Processing Systems*, 20, 465–472. Retrieved from <https://dl.acm.org/doi/10.5555/2981562.2981621>
- Fudenberg, D., Strack, P., & Strzalecki, T. (2018). Speed, accuracy, and the optimal timing of choices. *American Economic Review*, 108(12), 3651–3684. doi: 10.1257/aer.20150742
- Ghaderi-Kangavari, A., Amani Rad, J., & Nunez, M. D. (2023). A general integrative neurocognitive modeling framework to jointly describe EEG and decision-making on single trials. *Computational Brain & Behavior*, 6(3), 317–376. doi: 10.1007/s42113-023-00167-4
- Hadian Rasanan, A. H., Evans, N. J., Rieskamp, J., & Amani Rad, J. (2023). Numerical approximation of the first-passage time distribution of time-varying diffusion decision models: A mesh-free approach. *Engineering Analysis with Boundary Elements*, 151, 227–243. doi: 10.1016/jenganabound.2023.03.005
- Hawkins, G. E., Forstmann, B. U., Wagenmakers, E.-J., Ratcliff, R., & Brown, S. D. (2015). Revisiting the evidence for collapsing boundaries and urgency signals in perceptual decision-making. *Journal of Neuroscience*, 35(6), 2476–2484. doi: 10.1523/JNEUROSCI.2410-14.2015
- Murphy, P. R., Boonstra, E., & Nieuwenhuis, S. (2016). Global gain modulation generates time-dependent urgency during perceptual choice in humans. *Nature communications*, 7(1), 13526. doi: 10.1038/ncomms13526
- Murrow, M., & Holmes, W. (2024). A parameter recovery assessment of a wide class of evidence accumulation models of decision-making. *Preprint*. doi: 10.21203/rs.3.rs-4722049/v1
- Nunez, M. D., Gosai, A., Vandekerckhove, J., & Srinivasan, R. (2019). The latency of a visual evoked potential tracks the onset of decision making. *Neuroimage*, 197, 93–108. doi: 10.1016/j.neuroimage.2019.04.052
- Nunez, M. D., Schubert, A.-L., Frischkorn, G. T., & Oberauer, K. (2025). Cognitive models of decision-making with identifiable parameters: Diffusion decision models with within-trial noise. *PsyArXiv*. doi: 10.31234/osf.io/h4fde
- Ratcliff, R. (1978). A theory of memory retrieval. *Psychological Review*, 85(2), 59–108. doi: 10.1037/0033-295X.85.2.59
- Smith, P. L. (2000). Stochastic dynamic models of response time and accuracy: A foundational primer. *Journal of Mathematical Psychology*, 44(3), 408–463. doi: 10.1006/jmps.1999.1260
- Smith, P. L., & Ratcliff, R. (2022). Modeling evidence accumulation decision processes using integral equations: Urgency-gating and collapsing boundaries. *Psychological Review*, 129(2), 235–267. doi: 10.1037/rev0000301
- Tajima, S., Drugowitsch, J., & Pouget, A. (2016). Optimal policy for value-based decision-making. *Nature Communications*, 7(1), 12400. doi: 10.1038/ncomms12400
- Thura, D., Beauregard-Racine, J., Fradet, C.-W., & Cisek, P. (2012). Decision making by urgency gating: theory and experimental support. *Journal of neurophysiology*, 108(11), 2912–2930. doi: 10.1152/jn.01071.2011
- Weindel, G., Anders, R., Alario, F., & Burle, B. (2021). Assessing model-based inferences in decision making with single-trial response time decomposition. *Journal of Experimental Psychology: General*, 150(8), 1528–1555. doi: 10.1037/xge0001010
- Weindel, G., van Maanen, L., & Borst, J. P. (2024). Trial-by-trial detection of cognitive events in neural time-series. *Imaging Neuroscience*, 2, 1–28. doi: 10.1162/imag.a.00400